



Salt chemistry and Redox control

Jinsuo Zhang^{1,2}

- 1) Virginia Tech
- 2) Ohio State University

Research Team

- ❑ PI: Dr. Jinsuo Zhang, Dr. Shaoqiang Guo
- ❑ Students: Ryan Chesser, Yafei Wang (graduated from OSU, current Ph.D student of VT), Qiufeng Yang, Nik Shay (graduated), Bill Cohen (Graduated), Wentao Zhou (graduated), Evan Wu (graudated)
- ❑ Visiting Scholar: Dr. Wei Wu

All the experimental measurements presented were conducted at The Ohio State University

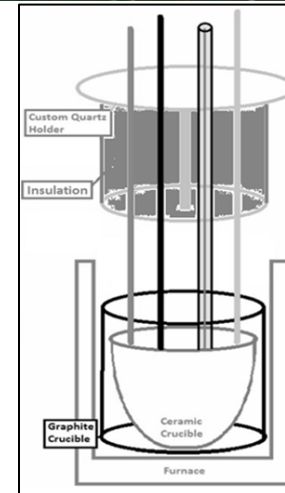
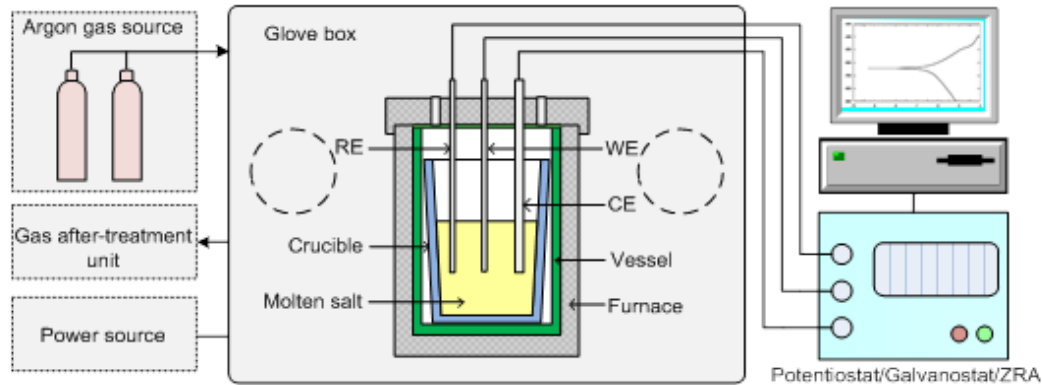
Salt impurities/source term

- Tritium
- Noble Gas (Xe, Kr)
- Noble metals (Nb, Mo, Tc, Ru, Rh, Ag, Cd, In, Sn, Zn, Ga, Ge, As)
- Halogens (I, Br)
- Tellurium Group (Te, Sb, Se)
- Barium, Strontium (Ba, Sr)
- Rare earth/alkaline metals (Y, La, Ce, Pr, Nd, Pm, Gd, Tb, Dy, Ho, Er, Zr, Sm, Eu, Sr, Ba, Rb, Cs)
- Actinide (U, Pu, Np)
- Corrosion Products (Ni, Fe, Cr)

What do we have to do

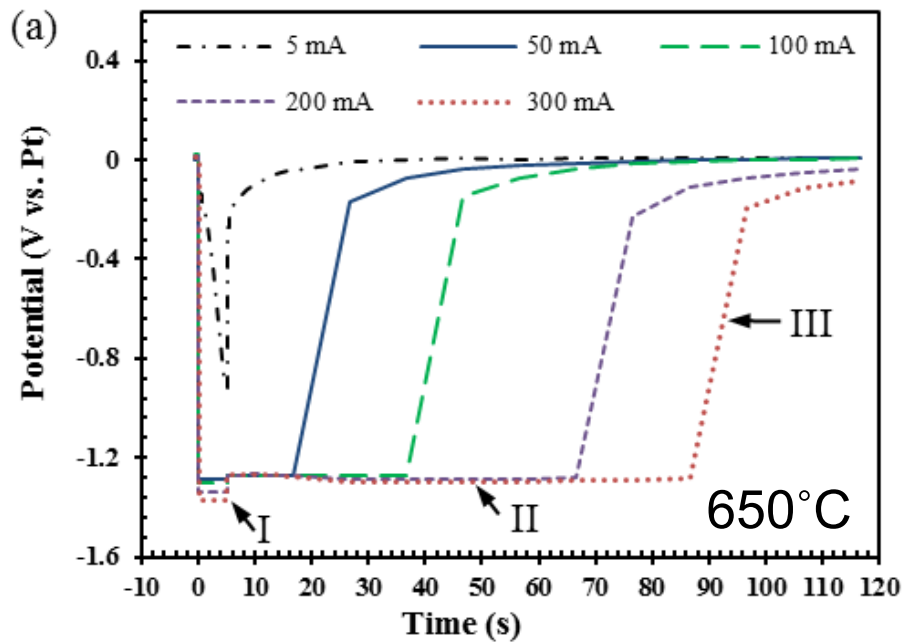
- Review the available data
- Measure fundamental data of element in the salt and liquid Bi
- Develop chemical (redox) control method
- Develop and design salt purification system in operation

Measurement-experimental set up



- ❑ A three-electrode system: working electrode (WE); Count electrode (CE) and Reference electrode (RE).
- ❑ Glove box (purged with Argon): the O_2 and H_2O was controlled below 4.0 during all experiments.
- ❑ Electrochemical technology: CV, EIS, LP, *etc*
- ❑ Properties measured: apparent potential, diffusion coefficient, activity coefficient, exchange current,

Determining of reference potential



Zone I: 5s current pulse is applied, and the potential of the W electrode becomes more negative due to the formation of a potassium layer on electrode surface. More negative potential at greater current due to the potential drop in electrolyte.

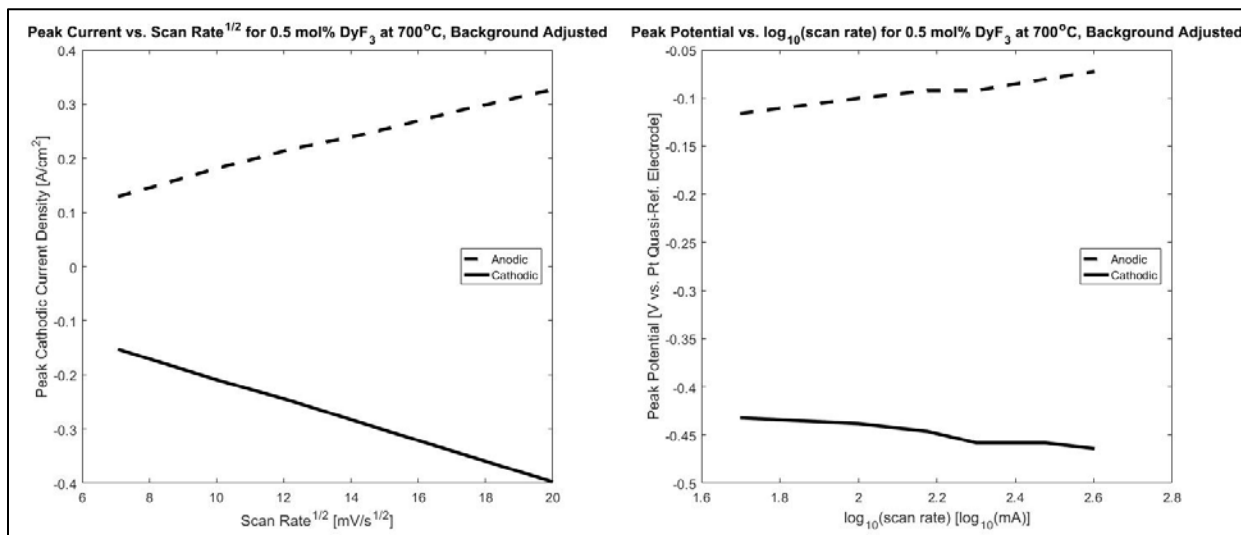
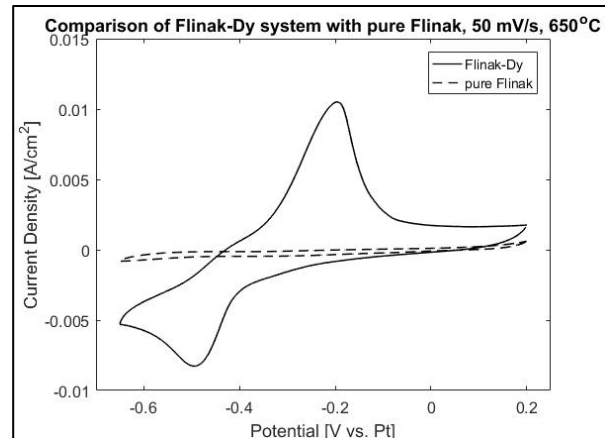
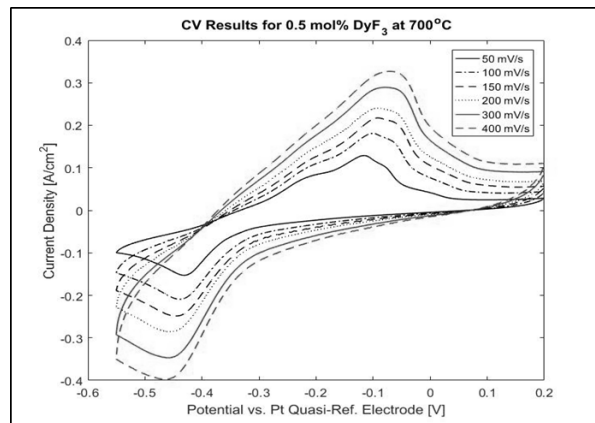
Zone II: No current applied. Consistent potential represents K^+/K potential.

Zone III: Potential returns back due to dissolution of K.

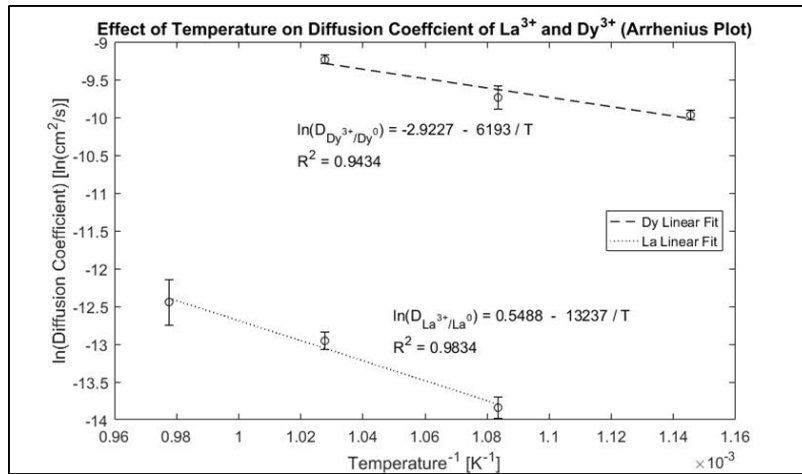
Temperature ($^{\circ}C$)	$E_{K^+/K}^{redox}$ (V vs. Pt)	Standard Deviation (mV)
650	-1.272	3.2
700	-1.270	2.9
750	-1.271	4.6

Electrolyte resistance of $0.12 \Omega \cdot cm^2$ at $650^{\circ}C$, $0.11 \Omega \cdot cm^2$ at $700^{\circ}C$ and $0.09 \Omega \cdot cm^2$ at $750^{\circ}C$

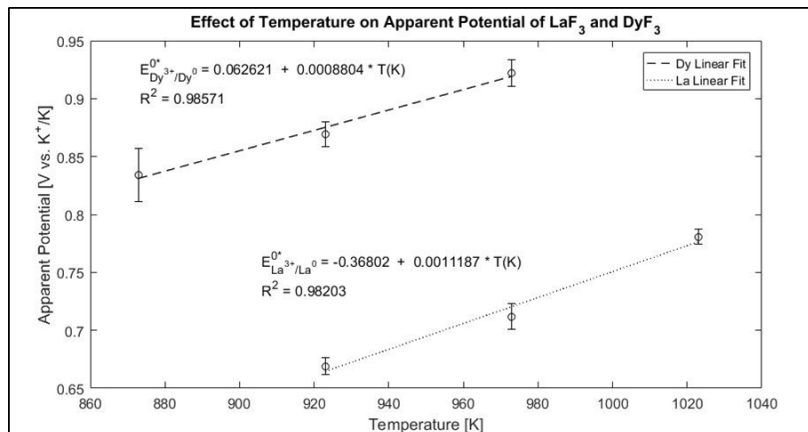
Measured CV signal



Diffusion coefficient and Apparent potential of Dy and La

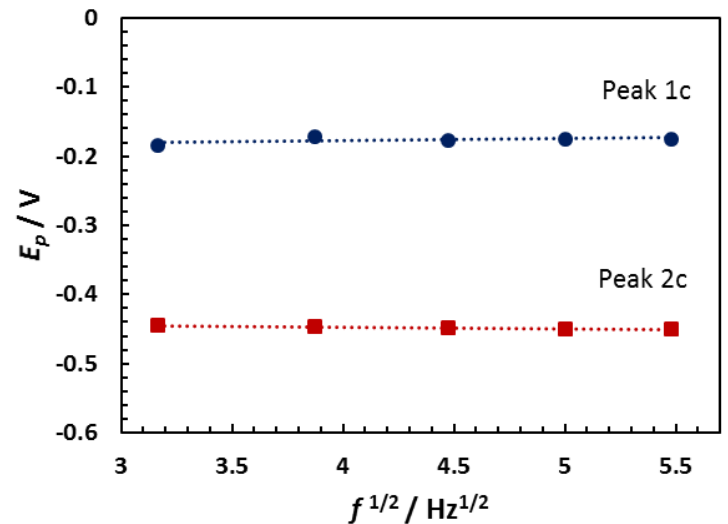
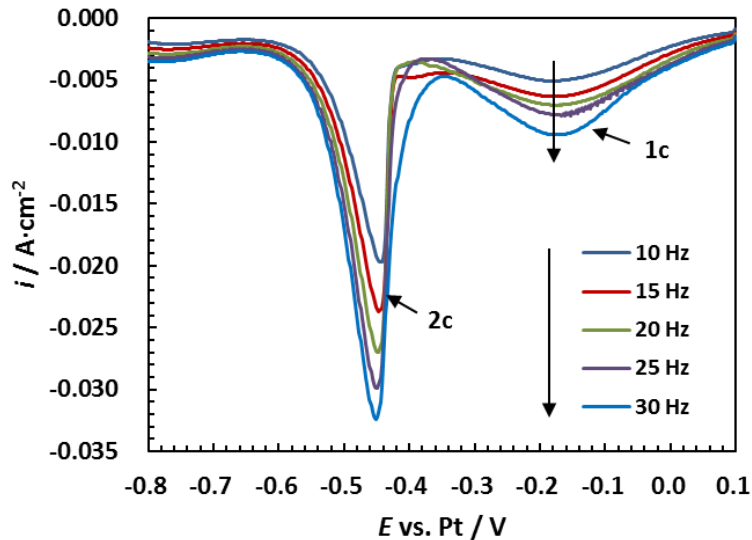
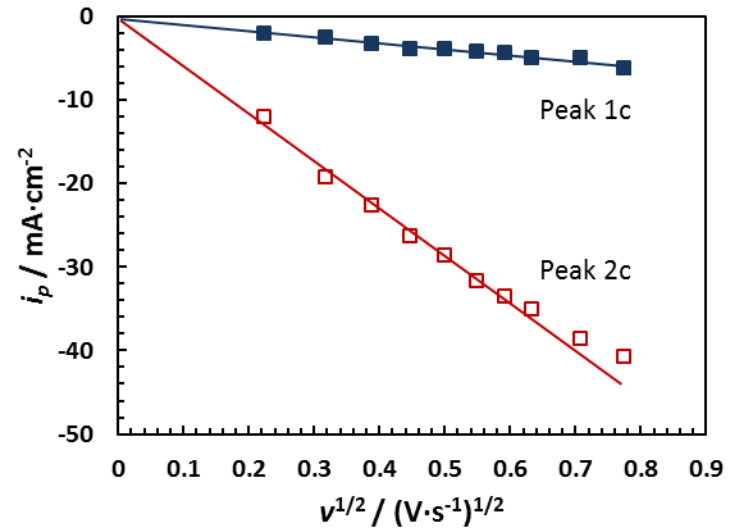
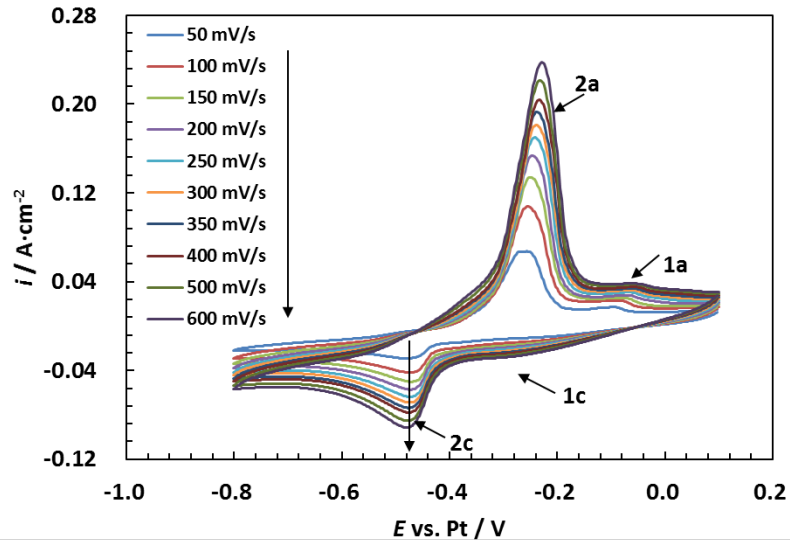


Diffusion activation energy: 51.5 kJ/mol for Dy³⁺, 127 kJ/mol for La³⁺



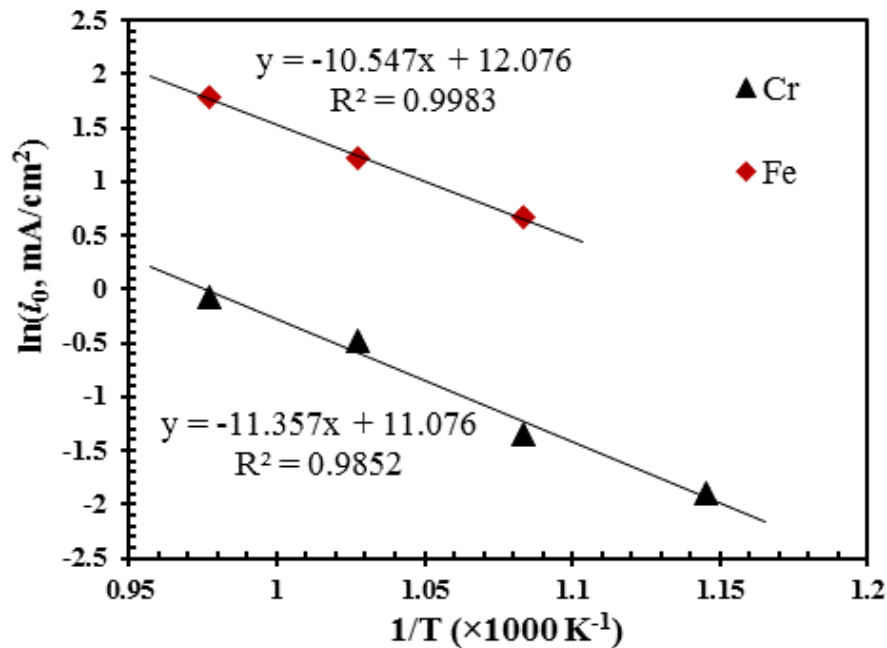
Both diffusion coefficient and apparent potential increases with temperature

Fundamental data of Corrosion Products



Exchange current density of Fe and Cr

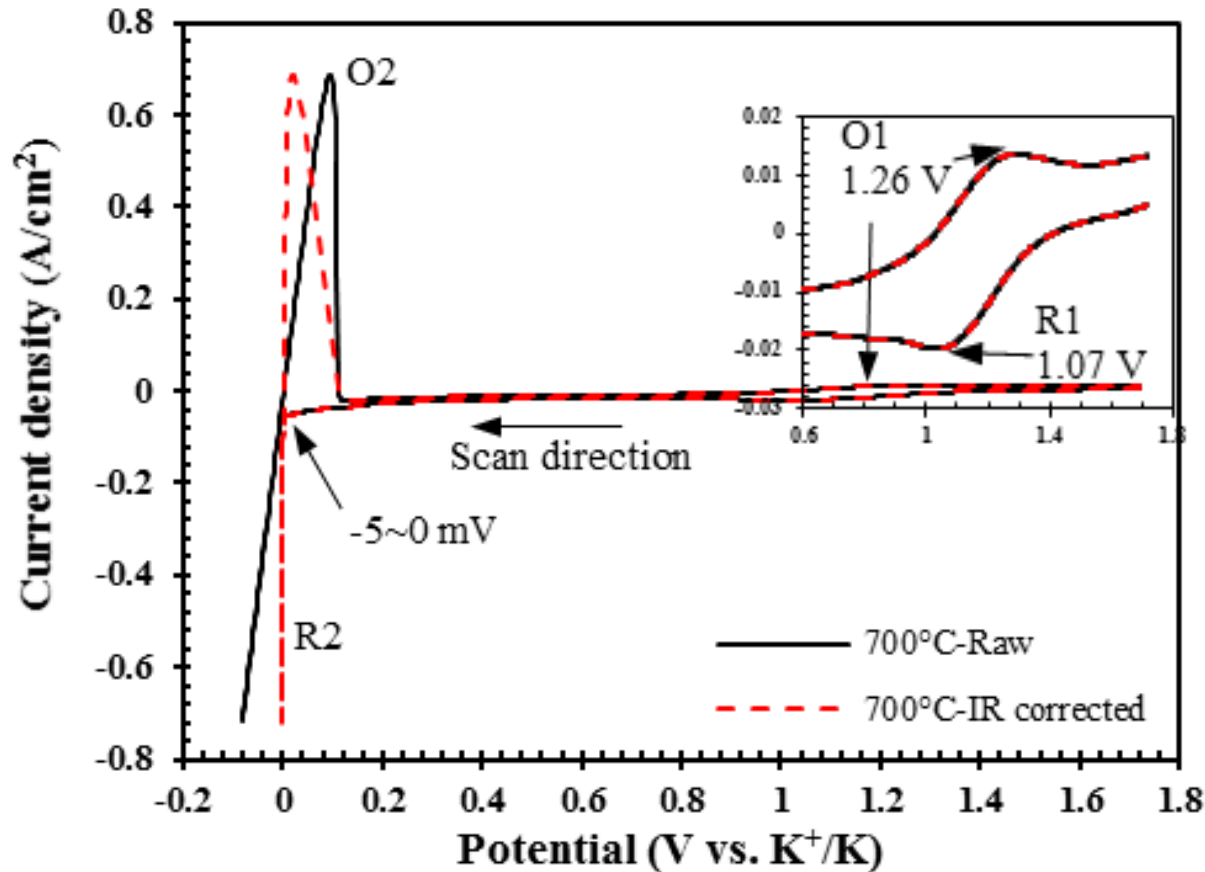
- Activation energy: 94.42 kJ/mol for Cr/Cr²⁺, and 87.69 kJ/mol for Fe/Fe²⁺ in molten FLiNaK



Redox Control

- Cover gas control method
- Metal control method
- Dissolved salt control method
- Refueling control method
- Cathodic protection

Dissolved Salt control method



Tungsten electrode, 700°C, FLiNaK-EuF₃-EuF₂, 200 mV/s

Concentration ratio of $\text{Eu}^{3+}/\text{Eu}^{2+}$

- Randles-Sevcik equation is not valid for system containing both members (e.g., both U^{4+} and U^{3+}) of the redox couple:

$$i_p = 0.4463nFC_bD^{1/2} \left(\frac{nFv}{RT} \right)^{1/2}$$

- Theory developed by Keightley et al. are adopted [1]:

- $\vec{i} = nF(C_b^{\text{Red}}D_{\text{Red}}^{1/2} + C_b^{\text{Ox}}D_{\text{Ox}}^{1/2}) \left(\frac{nFv}{RT} \right)^{1/2} \chi(\xi; \xi_i)$

- $\vec{i} = nF(C_b^{\text{Red}}D_{\text{Red}}^{1/2} + C_b^{\text{Ox}}D_{\text{Ox}}^{1/2}) \left(\frac{nFv}{RT} \right)^{1/2} [\chi(2\xi_r - \xi, \xi_i) - \chi(2\xi_r - \xi, \xi_r) - \chi(-\xi, \xi_r)]$

- where $\chi(x, \alpha) = \frac{d^{1/2}}{dx^{1/2}} \frac{1}{2\sqrt{\pi}} \left[\tanh\left(\frac{x+\alpha}{2}\right) - \tanh\left(\frac{\alpha}{2}\right) \right]$; $\xi = nF(E - E_{1/2})/RT$

[1] A.M. Keightley, et al, J. Electroanal. Chem. 322 (1992) 25-54.

Determined concentration ratio

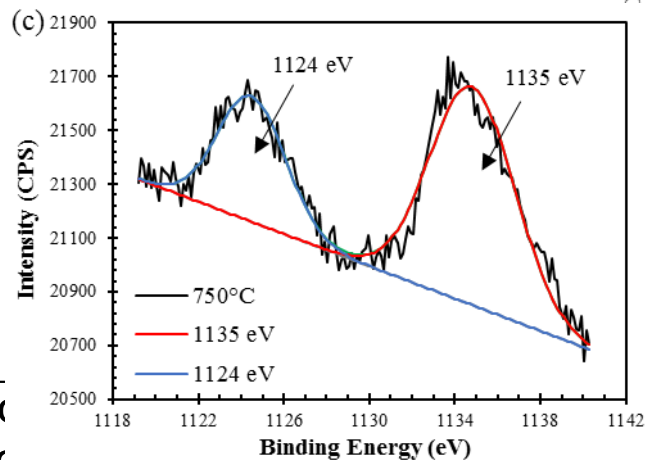
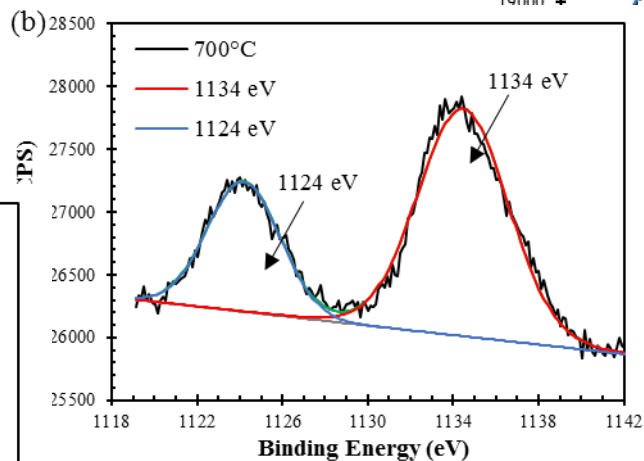
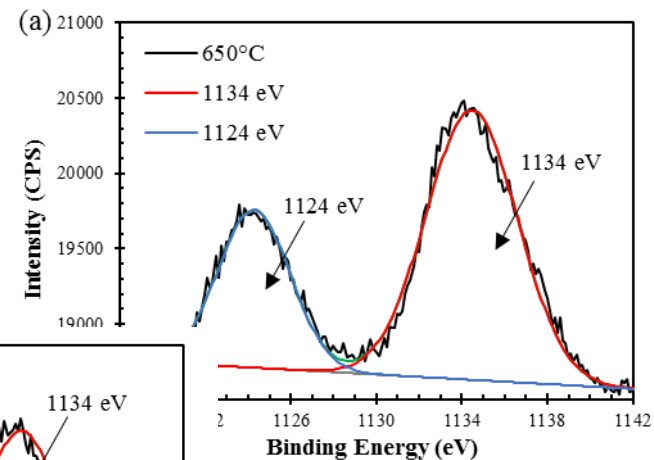
Predicted coordinates of cyclic voltammetric peaks and the calculated concentration ratio.

Test #	$\frac{nF}{RT} \Delta E_p$	$\frac{C_{Eu^{2+}}}{C_{Eu^{3+}}} \sqrt{\frac{D_{Eu^{2+}}}{D_{Eu^{3+}}}}$	$\frac{ i_p }{C^b} \sqrt{\frac{RT}{n^3 F^3 \nu D^b}}$	$\frac{nF}{RT} (E_{1/2} - E_p^c)$	$\frac{C_{Eu^{3+}}}{C_{Eu^{2+}}}$ †
-	2.236	0	0.4463	1.109	-
650°C #1	2.814	1.31	0.5415	1.697	1.21
650°C #2	3.102	2.13	0.5596	1.988	1.96
650°C #3	3.075	2.04	0.5581	1.959	1.88
700°C #1	2.855	1.42	0.5447	1.741	1.29
700°C #2	3.067	2.02	0.5578	1.953	1.83
700°C #3	3.119	2.18	0.5605	2.003	1.98
750°C #1	2.740	1.13	0.5356	1.623	1.08
750°C #2	2.674	0.98	0.5299	1.558	0.93
750°C #3	2.842	1.39	0.5439	1.729	1.33

†Calculated by the determined diffusion coefficient.

XPS examination

- $\text{Eu}^{3+}/\text{Eu}^{2+}$ ratio $\approx 2:1$



Formal potential for $\text{Eu}^{3+}/\text{Eu}^{2+}$

- $$E^* = E_{1/2} + \frac{RT}{nF} \ln \left(\frac{D_{\text{Ox}}}{D_{\text{Red}}} \right)^{\frac{1}{2}}$$

Table Summary of formal standard potential from this work and references

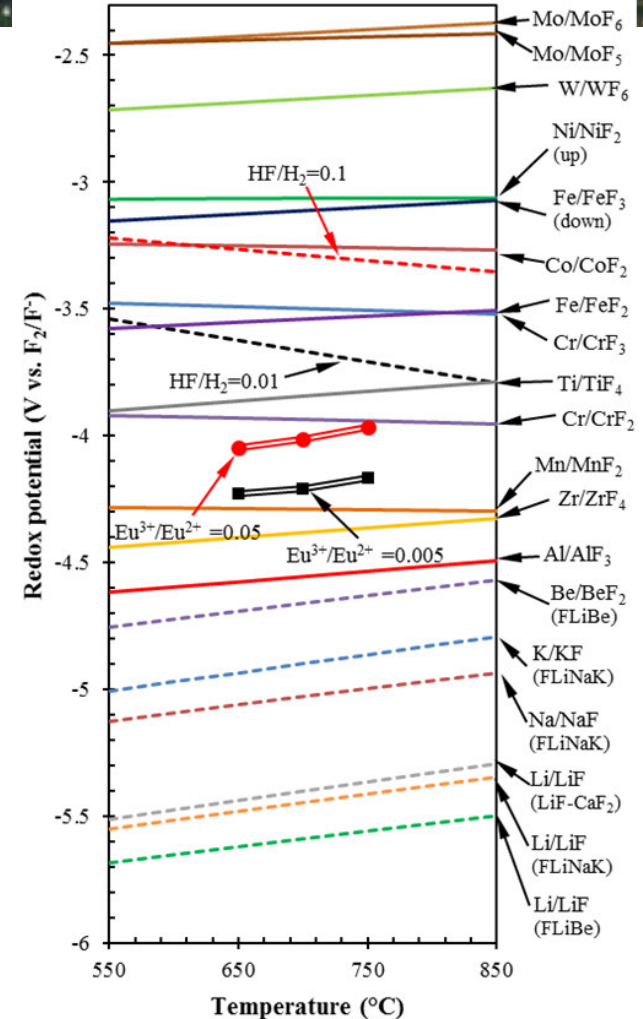
Temperature (° C)	E^* (V vs. F_2/F^-)	Salt	Total concentration of Eu in salt	Source
550	-3.94 or -3.82 [†]	FLiNaK	0.072 mol/kg	[1]
650	-3.836 ± 0.005	FLiNaK	0.048 mol/kg	This work
700	-3.787 ± 0.009	FLiNaK	0.048 mol/kg	This work
750	-3.732 ± 0.006	FLiNaK	0.048 mol/kg	This work
800	-3.53 ± 0.01	LiF-CaF ₂	0.100 mol/kg	[2]
820	-3.46 ± 0.01	LiF-CaF ₂	0.100 mol/kg	[2]
840	-3.40 ± 0.01	LiF-CaF ₂	0.100 mol/kg	[2]
870	-3.33 ± 0.01	LiF-CaF ₂	0.100 mol/kg	[2]

[1] W. Huang, et al. *Electrochimi. Acta* 147 (2014) 114-120.

[2] L. Massot, et al. *Electrochimi. Acta* 54 (2009) 6361-6366

Redox potential window

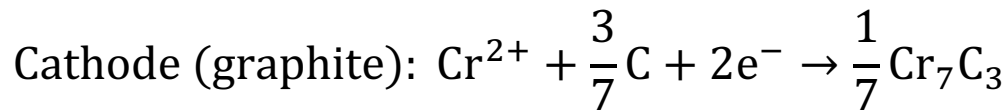
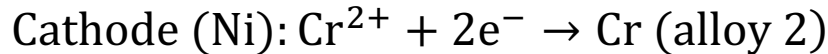
- Solid line: metal dissolution at limit activity of 10^{-6}
- Dotted line: reduction of oxidants. HF/H₂ = 0.1: a mole ratio of HF/H₂ = 0.1 at 1 atm total pressure
- Double solid line: redox potential calculated based on measured apparent potential.
- All potentials calculated based on ΔG° of fluorides at supercooled state except gaseous MoF₅, MoF₆, WF₆, and HF.



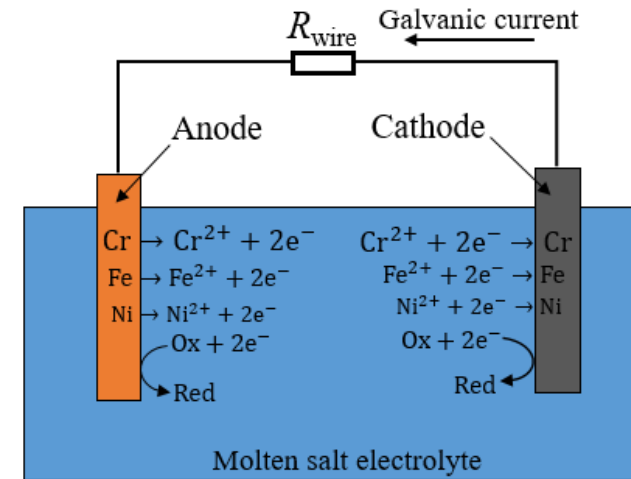
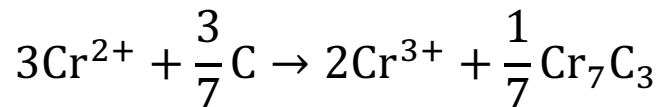
Acceleration mechanisms of Cr Dissolution

Galvanic Corrosion

Direct reduction of Cr^{2+}



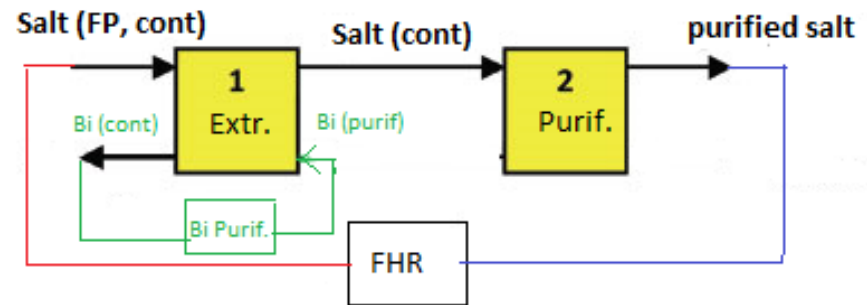
Disproportionation reaction of Cr^{2+}



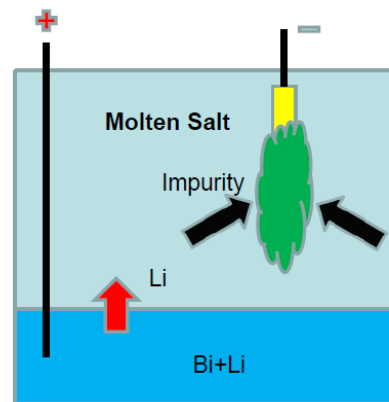
Schematic of the direct reduction of the corrosion products on the cathode during galvanic corrosion. Ox represents the residual oxidants.

Salt Purification Method

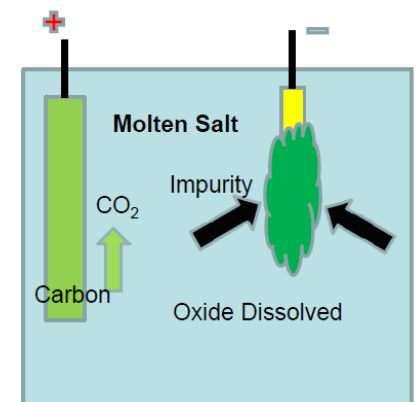
Bi-Li Extractor



Sacrificial Electrode



(a) Bi+Li sacrificial anode



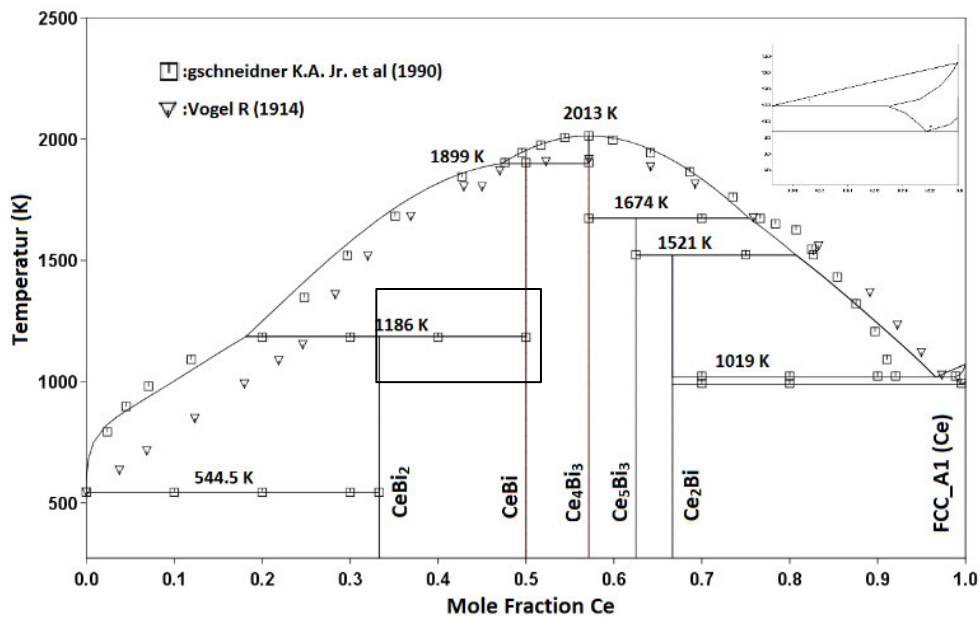
(b) Carbon sacrificial anode

Available Fundamental data in Liquid

Rare earth metals	Solid in equilibrium with the liquid	$\ln X_S = A - (B/T)$		Temperature range (K) (T_{\min} , T_{\max})	Reference	
		A	B			
Y	YBi	0.8549	6195	588–1000	(Schweitzer and Weeks, 1961b) ^a (Kober et al., 1971a)	
	YBi	-2.8783	5941			648–948
La	LaBi ₂	2.1359	5366	548–933	(Schweitzer and Weeks, 1961b) (Kober et al., 1968) Overall fitting ^a	
	LaBi ₂	5.8391	8044			648–948
	LaBi ₂	3.9875	6705			548–948
Ce	CeBi ₂	2.4958	5804	573–723	(Schweitzer and Weeks, 1961b) (Pleasance, 1959–1960) (Kober et al., 1971b) Overall fitting ^a	
	CeBi ₂	4.4073	6978			
	CeBi ₂	2.9748	6289			648–948
	CeBi ₂	2.7353	6046			573–948
Pr	PrBi ₂	0.4704	4502	548–623	(Schweitzer and Weeks, 1961b; Weeks, 1971) (Schweitzer and Weeks, 1961b)	
	PrBi ₂	3.3100	6287			623–723
Nd	NdBi ₂	2.2366	5873	573–773	(Schweitzer and Weeks, 1961b) (Smith, 1972a)	
	NdBi ₂	3.3813	6287			573–923
Sm	SmBi ₂	5.6721	7492	573–773	(Schweitzer and Weeks, 1961b)	
Eu	EuBi ₂	6.0346	6847	598–823	(Smith, 1972b)	
Ho	HoBi	-0.65	1818	673–873	(Antonchenko et al., 2009)	
Er	ErBi	2.7927	7054	775–975	(Petrashevich et al., 1976) (Yamshchikov et al., 1982) Overall fitting ^a	
	ErBi	1.0378	5509			890–1090
	ErBi	1.9153	6281			775–1090
Yb	YbBi ₂	4.6154	5527	553–673	(Weeks, 1965, 1971)	
Lu	Unknown	0.9790	6587	623–773	(Weeks, 1965, 1971)	

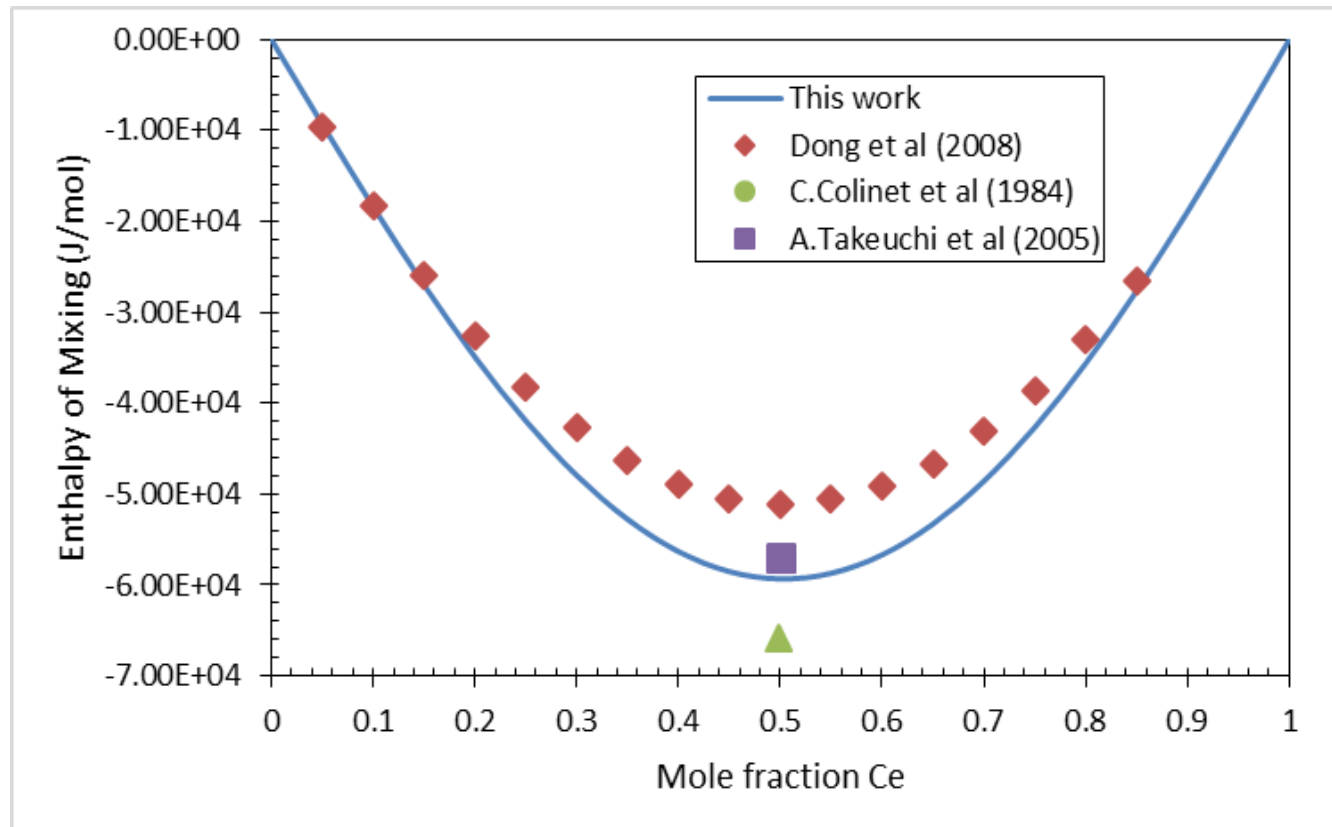
Rare earth metals	$\ln \gamma = A - (B/T)$		Temperature range (K) (T_{\min} , T_{\max})	Reference	
	A	B			
Y	-2.1049	16,502	673–773 773–1023	(Kurata et al., 1996) (Kober et al., 1971a)	
	0.8291	20,063			
La	1.9437	25,494	673–953	(Gschneidner and Calderwood, 1989a; Kober et al., 1968) (Castrillejo et al., 2007) (Kurata et al., 1996) (Yamana et al., 2001) Overall fitting ^a	
	3.8249	-26,750			653–823
	3.2836	-26,437			673–773
	3.3810	-26,646			850–1100
Ce	3.1083	-26,332	653–1100	(Kober et al., 1971b) (Kurata et al., 1996) (Castrillejo et al., 2007) (Yamana et al., 2001) (Dong et al., 2008a) Overall fitting ^a	
	4.6751	-26,254			773–923
	2.8145	-25,235			673–773
	3.7046	-26,089			653–823
	5.5280	-27,155			
Pr	2.3606	-25,612	735–937 653–937	(Kober et al., 1971b) (Kurata et al., 1996) (Castrillejo et al., 2007) (Yamana et al., 2001) (Dong et al., 2008a) Overall fitting ^a	
	3.8165	-26,067			653–937
	6.2425	-27,315			673–823
	2.8386	-24,994			673–773
	6.6995	-27,496			
Nd	7.6137	-28,554	673–823	(Castrillejo et al., 2005a, 2007) (Kurata et al., 1996) (Kober et al., 1985) (Lebedev, 1993) Overall fitting ^a	
	5.8486	-27,090			673–823
	5.1335	-26,470			
Sm	4.0293	-27,111		(Yamana et al., 2001; Lebedev, 1993)	
Eu	3.4520	-20,002		(Kurata et al., 1996; Lebedev et al., 1975)	
Gd			775–1055 850–1100	(Kurata et al., 1996; Dybinin et al., 1985) (Sheng et al., 2001a) (Yamana et al., 2001) (Lebedev, 1993) (Kober et al., 1983) (Kurata et al., 1996) Overall fitting ^a	
	3.1689	-23,060			
	4.4311	-24,326			
	3.7226	-24,163			
	2.8386	-22,697			
Tb	1.2268	-20,724	673–773 673–1100	(Kurata et al., 1996) Overall fitting ^a	
	3.0776	-22,994			
	4.6295	-24,035			850–1100
	4.6295	-24,035			850–1100
Dy	3.3305	-23,310	850–1100 850–1101	(Yamana et al., 2001) (Sheng et al., 2002) ^a	
	2.3099	-21,811			850–1101
Er	3.9391	-21,946	850–1100 773–973	(Yamana et al., 2001) (Gschneidner and Calderwood, 1989a)	
	-3.7677	-15,082			773–973

More fundamental data development based on phase diagram model



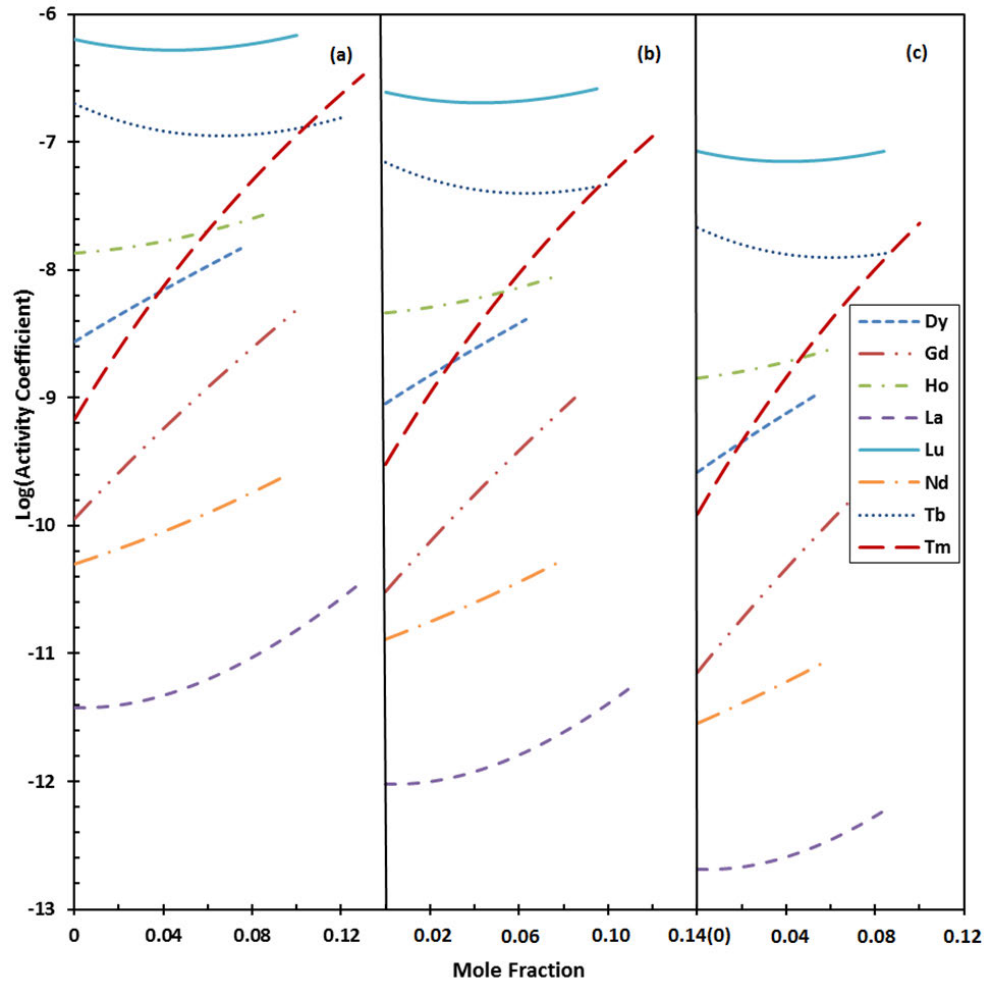
Bi-Ce

Fundamental data of Fission products in liquid Bi-Enthalpy of mixing



Bi-Ce

Activity coefficient of Fission products in liquid

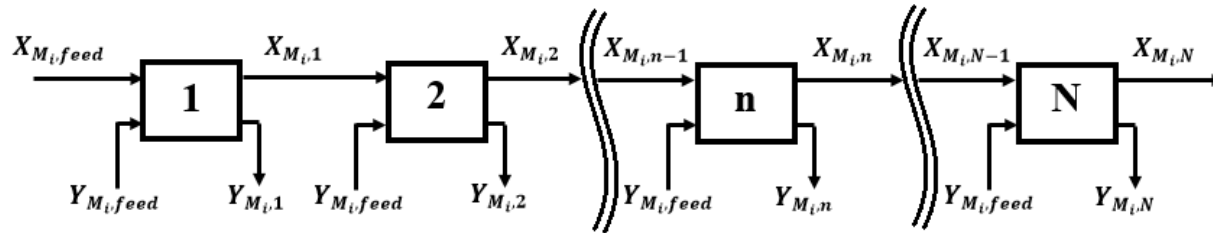


973 K

923 K

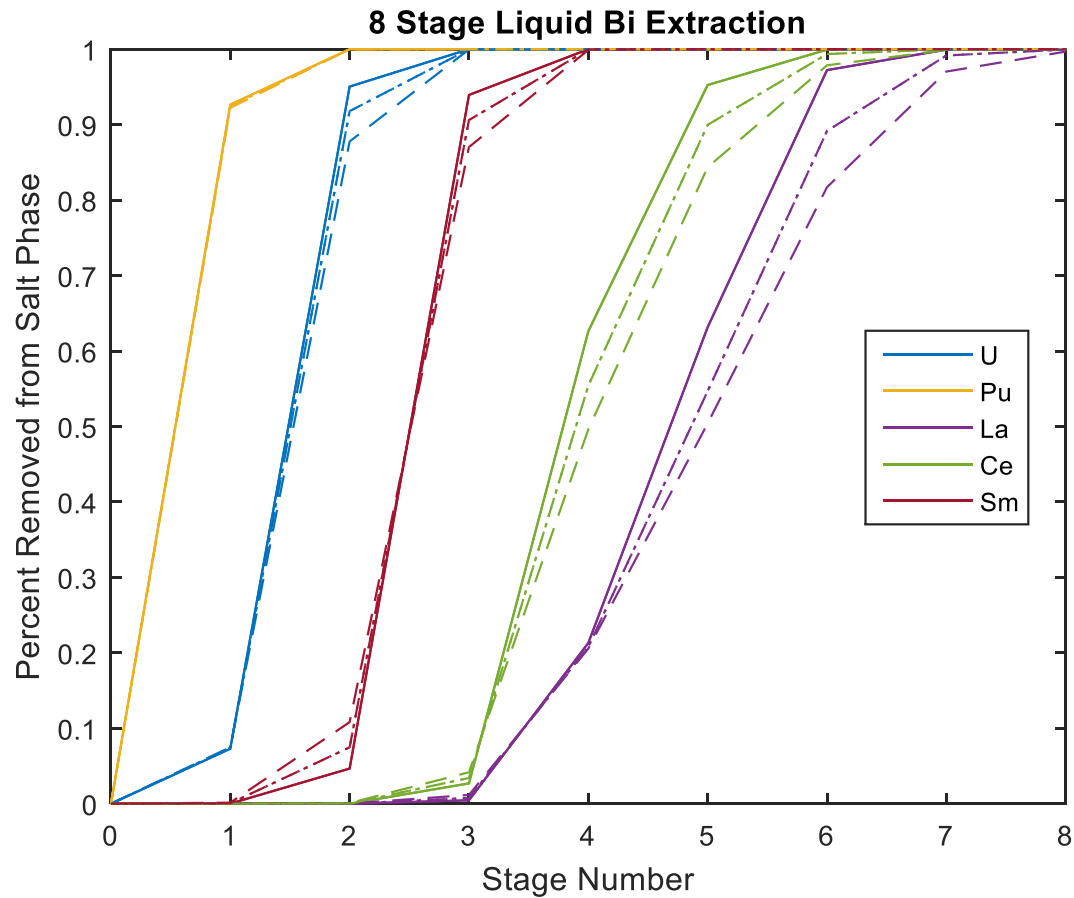
873 K

Purification model for Using Bi-Li

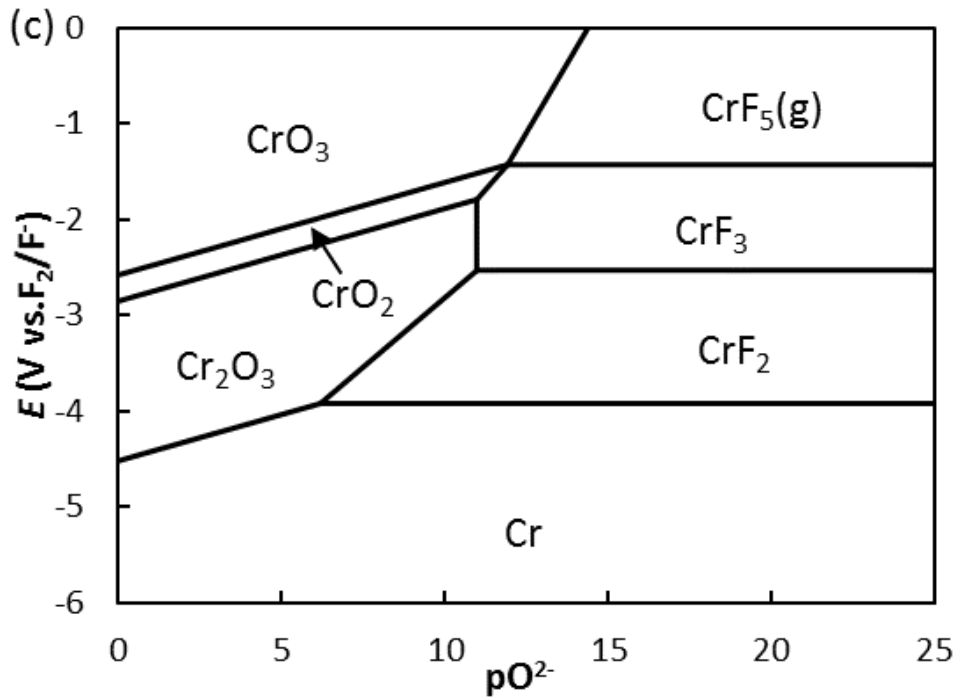


$$\sum_{i=1}^m \frac{n_i X_{M_i}^{I_{n_i+}}}{Bi_{feed} + Salt_{feed} D_{M_i}} = \frac{Y_{Li}^I D_{Li} - X_{Li}^I}{Bi_{feed} + Salt_{feed} D_{Li}}$$

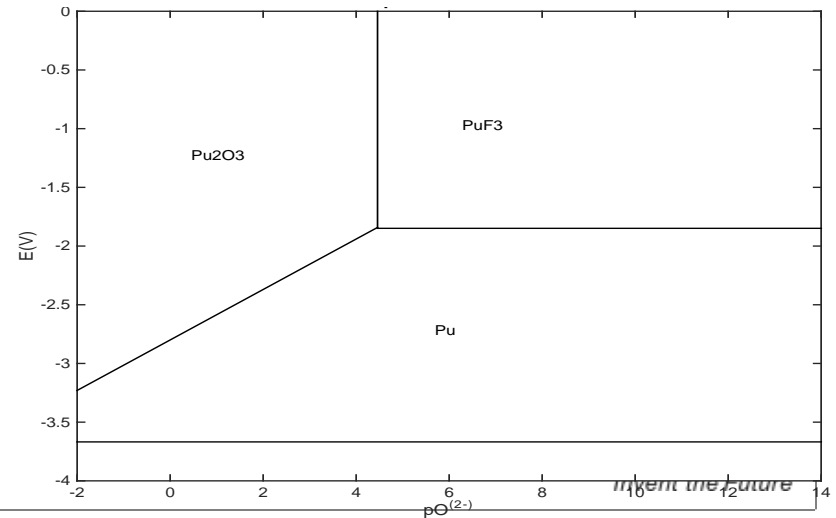
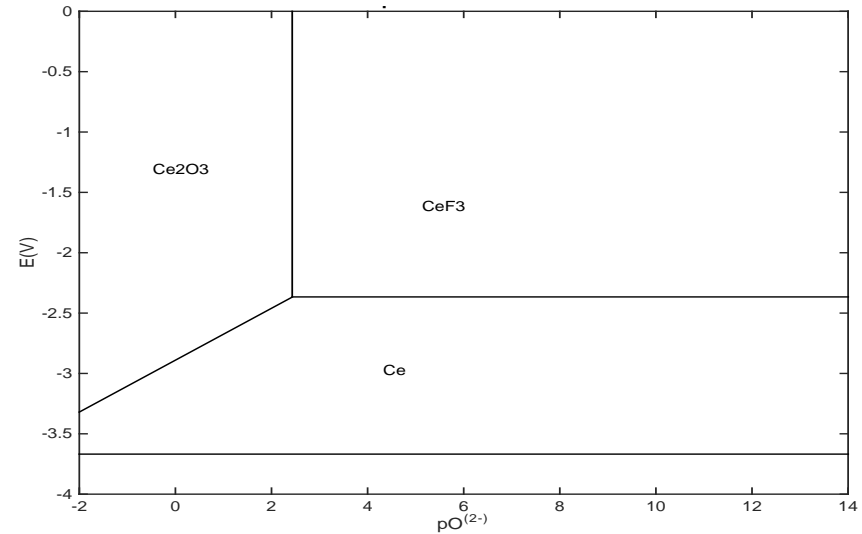
One Example



E-pO²⁻- diagram development

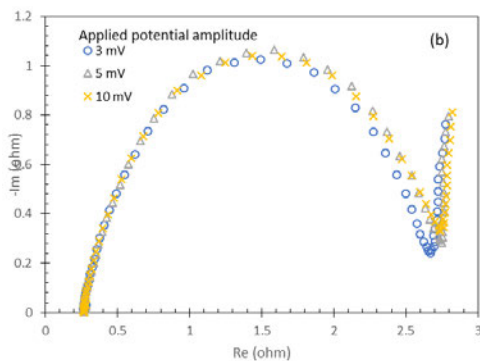


700C in FLiBe. $a_{M^{n+}}$ of 10^{-6} is used for the calculation of related equilibrium lines

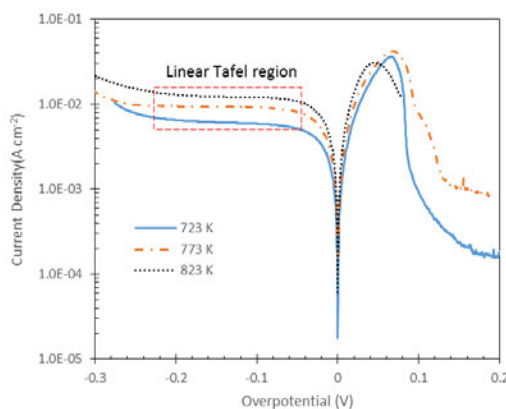


Chloride Salt Chemistry

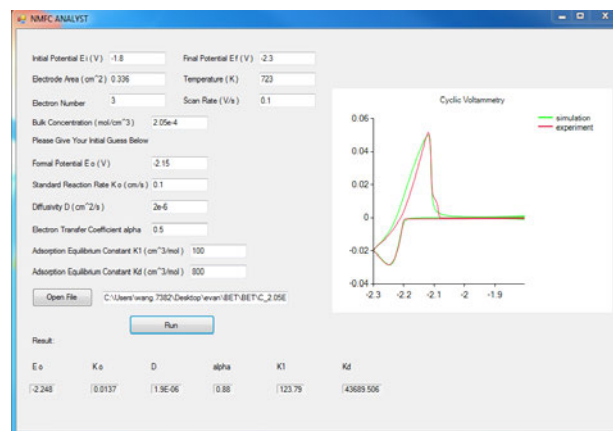
□ Nd, Gd, and La for high concentration up to 9wt% in KCl-LiCl



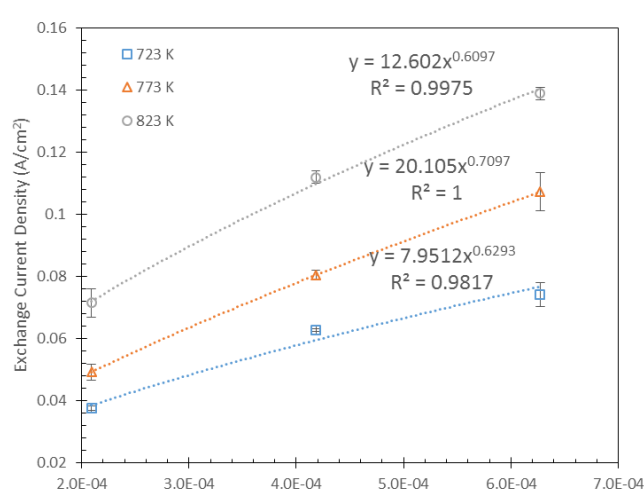
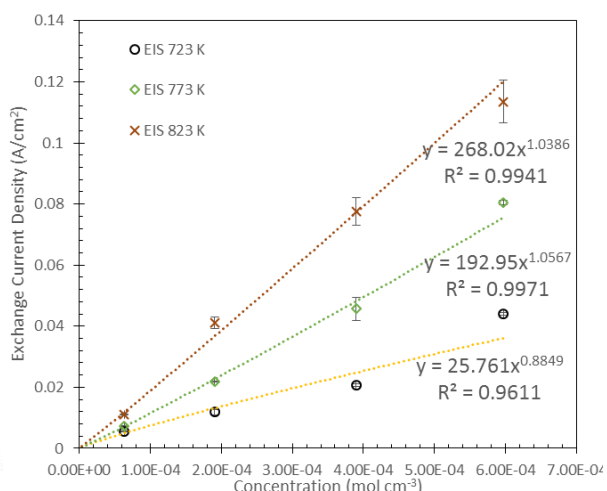
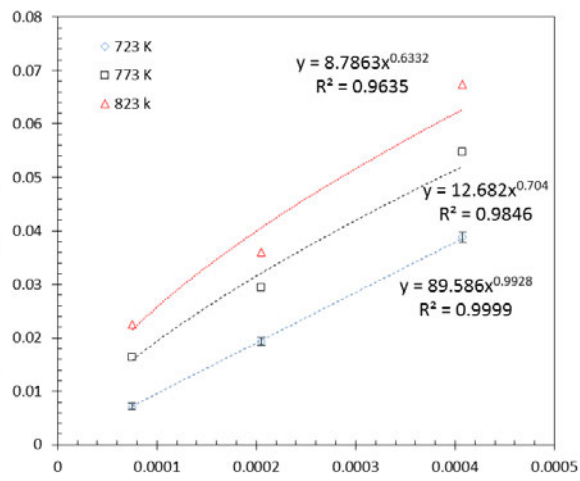
La³⁺



Gd³⁺



Nd²⁺



Questions?

